Available online at www.sciencedirect.com
SCIENCE DIRECT®
International Journal of Solids and Structures 42 (2005) 3487–3508
INTERNATIONAL JOURNAL OF SOLIDS and STRUCTURES
www.elsevier.com/locate/ijsolstr

Electroelastic field of a piezoelectric annular finite cylinder

R.K.N.D. Rajapakse [a,*], Y. Chen [a], T. Senjuntichai [b]

[a] *Department of Mechanical Engineering, The University of British Columbia, 2054-6250 Applied Science Lane, Vancouver, Canada V6T 1Z4*
[b] *Department of Civil Engineering, Chulalongkorn University, Bangkok 10330, Thailand*

Received 21 April 2004; received in revised form 5 October 2004
Available online 8 December 2004

Abstract

This paper presents a theoretical study of a piezoelectric annular cylinder under axisymmteric electromechanical loading. The piezoelectric material is assumed to be transversely isotropic and the general solutions of the governing equations are obtained in terms of a Fourier–Bessel series containing Bessel functions of the first and second kind. The boundary-value problems for vertical pressure and an electric charge loading applied to the ends of an annular cylinder are solved by expanding the applied loading in terms of a Fourier–Bessel series. Selected numerical results for the electroelastic field of an annular cylinder are presented for different aspect ratios of a cylinder and material properties.

Keywords: Cylinder; Elasticity; Electric field; Piezoelectricity; Stresses; Transversely isotropic material

1. Introduction

Piezoelectric elements are commonly used as sensors and actuators in adaptive structures (Matsuzaki, 1997). Piezoelectric materials generate an electric charge in response to mechanical deformations. Conversely, these materials produce mechanical strains under an applied electric field. Piezoelectric materials are available in a wide variety of shapes and sizes and can be distributed along a structure without greatly increasing its mass. Brittle behaviour and electric fatigue are two major concerns that limit industrial applications of piezoelectric materials. Among the many types of piezoelectric elements, the cylindrical (solid and hollow) shape is used in a broad range of practical applications such as resonators, actuators, fuel

* Corresponding author. Tel.: +1 6048220497; fax: +1 6048220944.
E-mail address: rajapakse@mech.ubc.ca (R.K.N.D. Rajapakse).

0020-7683/$ - see front matter © 2004 Elsevier Ltd. All rights reserved.
doi:10.1016/j.ijsolstr.2004.10.019

injectors, atomic force microscopes, high-precision telescopes, etc. The study of electroelastic field of a piezoelectric cylinder under combined electromechanical loading is therefore one of the fundamental problems of adaptive structures technology. Electric field and stress concentration in a cylindrical element could lead to dielectric breakdown, electrode delamination and fracture. Furthermore, tensile stresses due to applied loading could lead to tensile fracture as the tensile strength of these materials is relatively low.

Stress analysis of elastic solid and annular cylinders of infinite length is one of the fundamental problems in elasticity and has a rich history (Levin and Klosner, 1967; Atsumi and Itou, 1974; Kasano et al., 1982). The three-dimensional problem of a finite cylinder is much more complicated than that of an infinite cylinder. An isotropic finite cylinder under axial compression was analyzed by Pickett (1944) by using a multiple Fourier–Bessel series solution. A similar analysis for a constrained cylinder under end compression was done by Moghe and Neff (1971). Power and Childs (1971) presented a solution for an isotropic circular bar of finite length subjected to axi-symmetric tractions and/or displacements on either or both ends. The analysis of a transversely isotropic finite cylinder with a stress-free lateral surface was considered by Vendhan and Archer (1977) by using a displacement potential. Okumura (1987, 1989) used the generalized Elliott's solution (Elliott, 1948) to analyze a transversely isotropic, short hollow cylinder subjected to an outer band load. The analytic solutions for a finite transversely isotropic solid cylinder under different surface loads were presented by Wei et al. (1999); Chau and Wei (2000) and Wei and Chau (2002). These authors used the Lekhnitskii's stress functions (Lekhnitskii, 1963) to uncouple the equations of equilibrium. A new Fourier–Bessel series expansion of the stress function was proposed so that all boundary conditions can be exactly satisfied. It is noted here that study of free vibration of elastic cylinders was done long before the above studies dealing with cylinders under external static loading. Pochhammer in 1876 and Chree in 1889 determined the natural frequencies and mode shapes of an infinite ideal elastic cylinder (Love, 1944). Numerous other studies have followed the classical work of Pochhammer and Chree (Miklowitz, 1984). Hutchinson (1972, 1980) derived theoretical solutions for free vibrations of a finite elastic cylinder and presented a concise review of past studies related to free vibrations of infinite and finite cylinders.

Past studies on elastic cylinders provide a strong foundation for advancement of theoretical analysis of piezoelectric cylinders. Parton and Kudryavtsev (1988) present the general theory and solutions for a variety of problems of linear piezoelectricity. The classical solution of Pochhammer for flexural free vibrations of an infinite elastic cylinder was extended to the piezoelectric case by Paul (1966). The frequency equation becomes more complex for the piezoelectric case although the radial and vertical variations of the mode shapes are similar to the ideal elastic solution. Parton and Kudryavtsev (1988) presented the basic theory of wave propagation and considered a wide range of free vibration problems related to plates, cylinders and layered systems. They also presented an axisymmetric general solution for piezoelectricity by using Hankel integral transforms. Paul and Natarajan (1994a,b) considered the free vibration of a finite piezoelectric cylinder by extending the concepts proposed by Hutchinson (1972, 1980).

The study of infinite piezoelectric cylinders under external loading has received some attention in the past. Rajapakse (1996) and Rajapakse and Zhou (1997) used Fourier integral transforms to derive an analytic solution for an infinite piezoelectric cylinder and an infinite composite cylinder subjected to axisymmetric electromechanical loading. They examined the effects of coupling between mechanical and electric fields in a long cylinder and a composite cylinder and their solution can be easily extended to study the interaction between a piezoelectric fibre and a surrounding elastic medium.

A theoretical study of electromechanical response of a piezoelectric finite annular cylinder under externally applied mechanical and electric loading has not appeared in the literature. Therefore, the main objective of this study is to develop the analytical general solutions for a finite annular cylinder and examine the response of cylinders under some fundamental loading such as vertical pressure and electric charge loading applied to the ends of a cylinder. A set of potential functions are used to transform the governing equations expressed in terms of displacements and electric potential to a set of Laplace equations. The general solutions for Laplace equations are obtained in terms of a Fourier–Bessel series containing Bessel functions of

the first and second kind. Analytical general solution for the complete electroelastic field is presented and these solutions can be used to solve a wide range of boundary-value problems involving finite piezoelectric cylinders. The applied electromechanical loading of a cylinder is expressed in terms of a Fourier–Bessel series to determine the solutions for arbitrary functions appearing in the general solutions. Selected numerical results for different cylinder dimensions are presented for uniform vertical pressure and electric charge loading applied to the cylinder ends.

2. Analytical general solution

Fig. 1 shows a piezoelectric annular cylinder of inner radius a, outer radius b and height $2h$ under axisymmetric electromechanical loading applied to the boundary. A cylindrical polar coordinate system (r, θ, z) is used with the z-axis along the axis of symmetry of the cylinder. The cylinder is made out of a transversely isotropic piezoelectric material or a poled ceramic with the poling direction parallel to the z-axis.

The constitutive equations for piezoelectric materials which are transversely isotropic or poled along the z-axis can be expressed as (Parton and Kudryavtsev, 1988),

$$\sigma_{rr} = c_{11}\varepsilon_{rr} + c_{12}\varepsilon_{\theta\theta} + c_{13}\varepsilon_{zz} - e_{31}E_z \tag{1a}$$

$$\sigma_{\theta\theta} = c_{12}\varepsilon_{rr} + c_{11}\varepsilon_{\theta\theta} + c_{13}\varepsilon_{zz} - e_{31}E_z \tag{1b}$$

$$\sigma_{zz} = c_{13}\varepsilon_{rr} + c_{13}\varepsilon_{\theta\theta} + c_{33}\varepsilon_{zz} - e_{33}E_z \tag{1c}$$

$$\sigma_{rz} = 2c_{44}\varepsilon_{rz} - e_{15}E_r \tag{1d}$$

$$D_r = 2e_{15}\varepsilon_{rz} + \varepsilon_{11}E_r; \quad D_z = e_{31}\varepsilon_{rr} + e_{31}\varepsilon_{\theta\theta} + e_{33}\varepsilon_{zz} + \varepsilon_{33}E_z \tag{1e}$$

where σ_{ij}, ε_{ij}, D_i and E_i denote the components of stress tensor, strain tensor, electric displacement vector and electric field vector respectively; c_{11}, c_{12}, c_{13}, c_{33} and c_{44} are elastic constants under zero or constant electric field; e_{31}, e_{33} and e_{15} are piezoelectric constants; and ε_{11} and ε_{33} are dielectric constants under zero or constant strain.

The field equations for the axisymmetric case are

$$\frac{\partial\sigma_{rr}}{\partial r} + \frac{\partial\sigma_{rz}}{\partial z} + \frac{\sigma_{rr} - \sigma_{\theta\theta}}{r} = 0; \quad \frac{\partial\sigma_{rz}}{\partial r} + \frac{\partial\sigma_{zz}}{\partial z} + \frac{\sigma_{rz}}{r} = 0 \tag{2a}$$

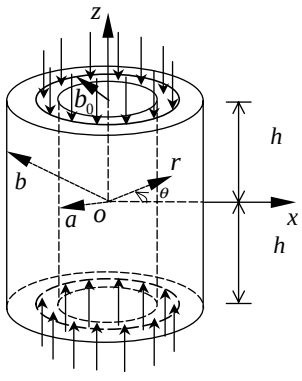

Fig. 1. Annular piezoelectric cylinder under vertical loading and the coordinate system.

$$\frac{\partial D_r}{\partial r}+\frac{\partial D_z}{\partial z}+\frac{D_r}{r}=0 \tag{2b}$$

Eq. (2a) represents the classical equilibrium equation in the absence of body forces and Eq. (2b) is the Gauss' equation representing the balance of electric flux in a charge-free medium. The strain–displacement relations are

$$\varepsilon_{rr}=\frac{\partial u_r}{\partial r};\quad \varepsilon_{\theta\theta}=\frac{u_r}{r};\quad \varepsilon_{zz}=\frac{\partial u_z}{\partial z};\quad \varepsilon_{zr}=\frac{1}{2}\left(\frac{\partial u_r}{\partial z}+\frac{\partial u_z}{\partial r}\right) \tag{3}$$

where u_r and u_z denote the displacements in the r- and z-directions respectively.

The relationship between the electric field E_i $(i=r,z)$ and the electric potential ϕ can be expressed as

$$E_r=-\frac{\partial\phi}{\partial r};\quad E_z=-\frac{\partial\phi}{\partial z} \tag{4}$$

To facilitate the derivation of the analytic solution, the following potential function representation is introduced (Rajapakse, 1996; Rajapakse and Zhou, 1997; Ding et al., 1996).

$$u_r=\frac{\partial\psi}{\partial r};\quad u_z=k_1\frac{\partial\psi}{\partial z};\quad \phi=\frac{c_{44}k_2}{e_{31}}\frac{\partial\psi}{\partial z} \tag{5}$$

where $\psi(r,z)$ denotes a potential function, and k_1 and k_2 are unknown constants to be determined.

Combination of Eqs. (1) to (5) leads to the following set of governing equations expressed in terms of $\psi(r,z)$.

$$c_{11}\left(\frac{\partial^2\psi}{\partial r^2}+\frac{1}{r}\frac{\partial\psi}{\partial r}\right)+[c_{44}+k_1(c_{13}+c_{44})+k_2(e_{31}+e_{15})]\frac{\partial^2\psi}{\partial z^2}=0 \tag{6a}$$

$$(c_{44}k_1+c_{13}+c_{44}+e_{15}k_2)\left(\frac{\partial^2\psi}{\partial r^2}+\frac{1}{r}\frac{\partial\psi}{\partial r}\right)+[c_{33}k_1+e_{33}k_2]\frac{\partial^2\psi}{\partial z^2}=0 \tag{6b}$$

$$(e_{15}k_1+e_{31}+e_{15}-\varepsilon_{11}k_2)\left(\frac{\partial^2\psi}{\partial r^2}+\frac{1}{r}\frac{\partial\psi}{\partial r}\right)+[e_{33}k_1-\varepsilon_{33}k_2]\frac{\partial^2\psi}{\partial z^2}=0 \tag{6c}$$

Before proceeding to solve the above governing equations, it is prudent to define a set of nondimensional field variables. Typical values of elastic, piezoelectric and dielectric constants of piezoelectric materials are different by many orders of magnitude and this could lead to precision and numerical instability problems during the calculation of numerical solutions. The coordinates r and z and the displacements u_r and u_z are nondimensionalized by the outer radius b which is set as the nondimensional unit length parameter. The stresses and elastic constants are nondimensionalized by c_{44}. The electric displacements and piezoelectric constants are nondimensionalized by e_{31}. For convenience, the nondimensional coordinates, displacements, stresses, electric displacements, elastic constants and piezoelectric constants are denoted by the same symbols without loss of generality. In addition, the following nondimensional quantities are introduced.

$$\overline{\phi}=\frac{e_{31}}{c_{44}b}\phi;\quad \overline{\psi}=\frac{\psi}{b^2};\quad \overline{\varepsilon}_{11}=\frac{c_{44}}{e_{31}^2}\varepsilon_{11};\quad \overline{\varepsilon}_{33}=\frac{c_{44}}{e_{31}^2}\varepsilon_{33} \tag{7}$$

Using the nondimensional quantities, Eqs. 5 and (6a)–(6c) are changed to:

$$u_r=\frac{\partial\overline{\psi}}{\partial r};\quad u_z=k_1\frac{\partial\overline{\psi}}{\partial z};\quad \overline{\phi}=k_2\frac{\partial\overline{\psi}}{\partial z} \tag{8a}$$

$$c_{11}\left(\frac{\partial^2\overline{\psi}}{\partial r^2}+\frac{1}{r}\frac{\partial\overline{\psi}}{\partial r}\right)+[1+k_1(1+c_{13})+k_2(1+e_{15})]\frac{\partial^2\overline{\psi}}{\partial z^2}=0 \tag{8b}$$

$$(k_1+c_{13}+1+e_{15}k_2)\left(\frac{\partial^2\overline{\psi}}{\partial r^2}+\frac{1}{r}\frac{\partial\overline{\psi}}{\partial r}\right)+[c_{33}k_1+e_{33}k_2]\frac{\partial^2\overline{\psi}}{\partial z^2}=0 \tag{8c}$$

$$(e_{15}k_1+1+e_{15}-\overline{\varepsilon}_{11}k_2)\left(\frac{\partial^2\overline{\psi}}{\partial r^2}+\frac{1}{r}\frac{\partial\overline{\psi}}{\partial r}\right)+[e_{33}k_1-\overline{\varepsilon}_{33}k_2]\frac{\partial^2\overline{\psi}}{\partial z^2}=0 \tag{8d}$$

All nondimensional material properties appearing in the above governing equations have similar orders of magnitude and k_1 and k_2 are also dimensionless constants. A nontrivial solution of Eqs. (8b)–(8d) exists if and only if,

$$\frac{1+(1+c_{13})k_1+(1+e_{15})k_2}{c_{11}}=\frac{c_{33}k_1+e_{33}k_2}{k_1+1+c_{13}+e_{15}k_2}=\lambda \tag{9a}$$

$$\frac{1+(1+c_{13})k_1+(1+e_{15})k_2}{c_{11}}=\frac{e_{33}k_1-\overline{\varepsilon}_{33}k_2}{e_{15}k_1+1+e_{15}-\overline{\varepsilon}_{11}k_2}=\lambda \tag{9b}$$

where λ is a dimensionless constant to be determined.

Eqs. (9a) and (9b) have three unknowns k_1, k_2 and λ. Eliminating k_1 and k_2 in Eqs. (9a) and (9b), the following cubic equation of λ is obtained.

$$\Omega_1\lambda^3+\Omega_2\lambda^2+\Omega_3\lambda+\Omega_4=0 \tag{10}$$

where the coefficients Ω_i $(i=1,2,3,4)$ are constants expressed in terms of material properties and are defined in the Appendix (Eq. (A.1)).

The three roots of Eq. (10) are denoted by $\lambda_i (i=1,2,3)$ with λ_1 assumed to be a positive real number and λ_2 and λ_3 are either positive real numbers or a pair of complex conjugates with positive real parts. For each root of Eq. (10), the Eqs. (9a) and (9b) yield the solutions for k_1 and k_2. It is convenient to denote the corresponding solutions by $k_{ij} (i=1,2; j=1,2,3)$ where the subscript j identifies the corresponding root λ_i.

In view of the three roots λ_i obtained from Eq. (10), the Eqs. (8b)–(8d) yield the solutions for the three potential functions $\overline{\psi}_i$ $(i=1,2,3)$ governed by,

$$\frac{\partial^2\overline{\psi}_i}{\partial r^2}+\frac{1}{r}\frac{\partial\overline{\psi}_i}{\partial r}+\lambda_i\frac{\partial^2\overline{\psi}_i}{\partial z^2}=0 \quad (i=1,2,3) \tag{11}$$

Assuming that roots λ_i are unequal, the solutions for potential function $\psi(r,z)$, elastic displacements and electric potential can be rewritten in terms of $\overline{\psi}_i$ by using Eqs. (8a) and (11) as

$$\overline{\psi}=\overline{\psi}_1+\overline{\psi}_2+\overline{\psi}_3 \tag{12a}$$

$$u_r=\frac{\partial}{\partial r}(\overline{\psi}_1+\overline{\psi}_2+\overline{\psi}_3); \quad u_z=k_{11}\frac{\partial\overline{\psi}_1}{\partial z}+k_{12}\frac{\partial\overline{\psi}_2}{\partial z}+k_{13}\frac{\partial\overline{\psi}_3}{\partial z} \tag{12b}$$

$$\overline{\phi}=k_{21}\frac{\partial\overline{\psi}_1}{\partial z}+k_{22}\frac{\partial\overline{\psi}_2}{\partial z}+k_{23}\frac{\partial\overline{\psi}_3}{\partial z} \tag{12c}$$

The solution for the potential function $\overline{\psi}$ for the general case that includes equal roots is given in Appendix (Eq. (A.2)) and the Eq. (12) can be accordingly modified.

Eq. (11) can be expressed in the following form.

$$\frac{\partial^2\overline{\psi}_i}{\partial r^2}+\frac{1}{r}\frac{\partial\overline{\psi}_i}{\partial r}+\frac{\partial^2\overline{\psi}_i}{\partial z_i^2}=0 \quad (i=1,2,3) \tag{13}$$

where $z_i = z/\sqrt{\lambda_i}$.

The solution of Eq. (13) is given by (Bland, 1961),

$$\overline{\psi}_i = [AJ_0(tr)+BY_0(tr)][C_i\cosh(tz_i)+F_i\sinh(tz_i)] \quad (i=1,2,3) \tag{14}$$

where $J_0(tr)$ and $Y_0(tr)$ are Bessel functions of the first and the second kind of zero order, respectively (Bland, 1961); $\cosh(tz_i)$ and $\sinh(tz_i)$ are hyperbolic cosine and sine functions, respectively; and t, A, B, C_i and F_i $(i=1,2,3)$ are arbitrary functions to be determined.

On the other hand, Eq. (11) can also be expressed in the following form.

$$\frac{\partial^2\overline{\psi}_i}{\partial r_i^2}+\frac{1}{r_i}\frac{\partial\overline{\psi}_i}{\partial r_i}+\frac{\partial^2\overline{\psi}_i}{\partial z^2}=0 \quad (i=1,2,3) \tag{15}$$

where $r_i = \sqrt{\lambda_i}r$.

The solution of Eq. (15) is given by (Bland, 1961),

$$\overline{\psi}_i = [G_iI_0(sr_i)+L_iK_0(sr_i)][P\cos(sz)+R\sin(sz)] \quad (i=1,2,3) \tag{16}$$

where $I_0(sr_i)$ and $K_0(sr_i)$ are the modified Bessel functions of the first and second kind of zero order, respectively (Bland, 1961); and s, G_i, L_i, P and $R(i=1,2,3)$ are arbitrary functions to be determined. Therefore, the general solution of Eq. (11) can be expressed as,

$$\begin{aligned}\overline{\psi}_i = {} & [AJ_0(tr)+BY_0(tr)][C_i\cosh(tz_i)+F_i\sinh(tz_i)] \\ & +[G_iI_0(sr_i)+L_iK_0(sr_i)][P\cos(sz)+R\sin(sz)] \quad (i=1,2,3)\end{aligned} \tag{17}$$

For the axisymmetric case, the potential function should contain only even functions of z. In addition to the solution given by Eq. (17), it is necessary to include the potential functions for the radially symmetric plane problem of an annular cylinder and that of a long bar for the completeness of the general solution. Therefore, the complete general solution of the potential function $\overline{\psi}$ in Eq. (8a) can be expressed as,

$$\begin{aligned}\overline{\psi} = {} & B_{01}\ln r+\sum_{i=1}^{3}A_{0i}(r^2-2z_i^2) \\ & +\sum_{i=1}^{3}\left\{\sum_{m=1}^{\infty}[A_{im}J_0(t_mr)+B_{im}Y_0(t_mr)]\cosh(t_mz_i)+\sum_{n=1}^{\infty}[G_{in}I_0(s_nr_i)+L_{in}K_0(s_nr_i)]\cos(s_nz)\right\}\end{aligned} \tag{18}$$

where $s_n = \frac{n\pi}{h}$ and $A_{im}, B_{im}, G_{in}, L_{in}, A_{0i}$ $(i=1,2,3)$ and B_{01} are arbitrary functions and t_m is a constant. These unknown quantities have to be determined from the boundary conditions.

To facilitate the solution of boundary-value problems, the general solutions for displacements, stresses, etc. are expressed as sum of three parts: (a) the first part denoted by superscript '0' corresponds to the first two terms of the right hand side of Eq. (18); (b) the second part denoted by superscript '1' corresponds to the series containing the Bessel functions of the first and the second kind in Eq. (18); (c) the third part denoted by superscript '2' corresponds to the series containing modified Bessel functions of the first and the second kind in Eq. (18).

The corresponding general solutions of displacements and electric potential are:

$$u_r^{(0)}(r) = \frac{1}{r}B_{01}+2\sum_{i=1}^{3}A_{0i}r; \quad u_z^{(0)}(z) = -4\sum_{i=1}^{3}k_{1i}\frac{A_{0i}}{\lambda_i}z; \quad \overline{\phi}^{(0)}(z) = -4\sum_{i=1}^{3}k_{2i}\frac{A_{0i}}{\lambda_i}z \tag{19a}$$

$$u_r^{(1)}(r,z) = -\sum_{i=1}^{3}\sum_{m=1}^{\infty} t_m[A_{im}J_1(t_m r) + B_{im}Y_1(t_m r)]\cosh(t_m z_i) \tag{19b}$$

$$u_z^{(1)}(r,z) = \sum_{i=1}^{3} k_{1i}\sum_{m=1}^{\infty} \frac{t_m}{\sqrt{\lambda_i}}[A_{im}J_0(t_m r) + B_{im}Y_0(t_m r)]\sinh(t_m z_i) \tag{19c}$$

$$\overline{\phi}^{(1)}(r,z) = \sum_{i=1}^{3} k_{2i}\sum_{m=1}^{\infty} \frac{t_m}{\sqrt{\lambda_i}}[A_{im}J_0(t_m r) + B_{im}Y_0(t_m r)]\sinh(t_m z_i) \tag{19d}$$

$$u_r^{(2)}(r,z) = \sum_{i=1}^{3}\sum_{n=1}^{\infty} \sqrt{\lambda_i}s_n[G_{in}I_1(s_n r_i) - L_{in}K_1(s_n r_i)]\cos(s_n z) \tag{19e}$$

$$u_z^{(2)}(r,z) = -\sum_{i=1}^{3} k_{1i}\sum_{n=1}^{\infty} s_n[G_{in}I_0(s_n r_i) + L_{in}K_0(s_n r_i)]\sin(s_n z) \tag{19f}$$

$$\overline{\phi}^{(2)}(r,z) = -\sum_{i=1}^{3} k_{2i}\sum_{n=1}^{\infty} s_n[G_{in}I_0(s_n r_i) + L_{in}K_0(s_n r_i)]\sin(s_n z) \tag{19g}$$

The general solutions of stresses and electric displacements are given in the Appendix (Eqs. (A.3)–(A15)). According to authors' knowledge the above general solution for a piezoelectric finite annular cylinder is a new contribution. The general solution for a solid cylinder can be obtained by setting the terms containing Bessel functions of the second kind and modified Bessel functions of the second kind to zero.

3. Electromechanical loading of annular cylinder

In this section an annular cylinder subjected to two basic cases of electromechanical loading is analyzed by using the general solutions derived in the preceding section. First consider the case of a cylinder under normal pressure applied to the top and bottom ends (Fig. 1). Assume that all surfaces of the cylinder are electrically impermeable and the inner and outer cylindrical surfaces are stress free.

The boundary conditions can be expressed as follows:

$$\sigma_{rr}(a,z) = 0, \quad \sigma_{rz}(a,z) = 0, \quad D_r(a,z) = 0 \quad \text{for} \quad -h \leqslant z \leqslant h \tag{20a}$$

$$\sigma_{rr}(1,z) = 0, \quad \sigma_{rz}(1,z) = 0, \quad D_r(1,z) = 0 \quad \text{for} \quad -h \leqslant z \leqslant h \tag{20b}$$

$$\sigma_{zz}(r,\pm h) = -p(r), \quad \sigma_{zr}(r,\pm h) = 0, \quad D_z(r,\pm h) = 0 \quad \text{for } a \leqslant r \leqslant 1 \tag{20c}$$

where $p(r)$ denotes the nondimensional intensity of the normal pressure applied on the top and bottom surfaces of the cylinder.

The boundary conditions expressed by Eqs. (20a)–(20c) have to be used to determine the arbitrary functions A_{im}, B_{im}, G_{in} and $L_{in}(i = 1,2,3;\ m,n = 1,2,\ldots,\infty)$ appearing in the general solutions. Given the complexity of the analytical general solutions, it is prudent to apply the boundary conditions in a systematic way to solve for the arbitrary functions. First consider the boundary condition $\sigma_{zr} = 0$ at $z = \pm h$. Noting that $\sigma_{zr}^{(0)}$ and $\sigma_{zr}^{(2)}$ vanish at $z = \pm h$, the boundary condition, $\sigma_{zr} = \sigma_{zr}^{(0)} + \sigma_{zr}^{(1)} + \sigma_{zr}^{(2)} = 0$, is reduced to $\sigma_{zr}^{(1)} = 0$. Then using Eq. (A.8) and noting that this boundary condition has to be satisfied for $a \leqslant r \leqslant 1$, the following relationships can be obtained.

$$\sum_{i=1}^{3}\vartheta_i\sum_{m=1}^{\infty}A_{im}\sinh(t_m h_i)=0;\quad \sum_{i=1}^{3}\vartheta_i\sum_{m=1}^{\infty}B_{im}\sinh(t_m h_i)=0 \tag{21}$$

where $h_i = h/\sqrt{\lambda_i}$.

Using Eq. (21), express A_{1m} in terms of A_{2m} and A_{3m}, and B_{1m} in terms of B_{2m} and B_{3m} as

$$A_{1m}=\alpha_{1m}A_{2m}+\alpha_{2m}A_{3m};\quad B_{1m}=\alpha_{1m}B_{2m}+\alpha_{2m}B_{3m} \tag{22}$$

where

$$\alpha_{1m}=-\frac{\vartheta_2\sinh(t_m h_2)}{\vartheta_1\sinh(t_m h_1)};\quad \alpha_{2m}=-\frac{\vartheta_3\sinh(t_m h_3)}{\vartheta_1\sinh(t_m h_1)} \tag{23}$$

Substitution of Eq. (22) into Eq. (A.8) leads to,

$$\begin{aligned}\sigma_{zr}^{(1)}(r,z)=-\sum_{m=1}^{\infty}t_m^2\{&[\vartheta_1\sinh(t_m z_i)\alpha_{1m}+\vartheta_2\sinh(t_m z_i)][J_1(t_m r)A_{2m}+Y_1(t_m r)B_{2m}]\\&+[\vartheta_1\sinh(t_m z_i)\alpha_{2m}+\vartheta_3\sinh(t_m z_i)][J_1(t_m r)A_{3m}+Y_1(t_m r)B_{3m}]\}\end{aligned} \tag{24}$$

Noting that the shear stress boundary conditions on the inner and outer cylindrical surfaces ($r=a,1$) have to be satisfied for $-h\leqslant z\leqslant h$, the following conditions can be established.

$$\sigma_{rz}^{(1)}(a,z)=0;\quad \sigma_{rz}^{(2)}(a,z)=0;\quad \sigma_{rz}^{(1)}(1,z)=0;\quad \sigma_{rz}^{(2)}(1,z)=0 \tag{25}$$

Substituting the first condition of Eq. (25) in Eq. (24) yields,

$$A_{2m}=-\frac{Y_1(t_m a)}{J_1(t_m a)}B_{2m};\quad A_{3m}=-\frac{Y_1(t_m a)}{J_1(t_m a)}B_{3m} \tag{26}$$

Then substituting Eq. (26) into Eq. (24) and imposing the third condition of Eq. (25) yields the following transcendental equation to determine t_m.

$$J_1(t_m)Y_1(t_m a)-J_1(t_m a)Y_1(t_m)=0 \tag{27}$$

The arbitrary functions G_{1n} and G_{2n} can now be expressed in terms of G_{3n} and $L_{in}(i=1,2,3)$ by substituting the second and fourth boundary conditions of Eq. (25) in Eq. (A.13). Therefore,

$$G_{1n}=\frac{[\gamma_2(a)\xi_0-\gamma_3(a)]G_{3n}+\sum_{i=1}^{3}[\gamma_2(a)\xi_i+\kappa_i(a)]L_{in}}{\gamma_1(a)} \tag{28a}$$

$$G_{2n}=-\left(\xi_0 G_{3n}+\sum_{i=1}^{3}\xi_i L_{in}\right) \tag{28b}$$

where

$$\gamma_i(r)=\vartheta_i\lambda_i I_1(s_n r_i);\quad \kappa_i(r)=\vartheta_i\lambda_i K_1(s_n r_i)\quad (i=1,2,3) \tag{29a}$$

$$\xi_0=\frac{\gamma_1(a)\gamma_3(1)-\gamma_1(1)\gamma_3(a)}{\gamma_1(a)\gamma_2(1)-\gamma_1(1)\gamma_2(a)};\quad \xi_i=\frac{\gamma_1(1)\kappa_i(a)-\gamma_1(a)\kappa_i(1)}{\gamma_1(a)\gamma_2(1)-\gamma_1(1)\gamma_2(a)}\quad (i=1,2,3) \tag{29b}$$

Until now only shear stress boundary condition of the cylinder has been used ($\sigma_{zr}=0$ at $r=a,1$ and $z=\pm h$) and the unknowns $A_{1m}, A_{2m}, A_{3m}, B_{1m}, G_{1n}$ and G_{2n} are expressed in terms of the remaining arbitrary constants.

Next, consider the normal stress and normal electric displacement boundary conditions given by Eq. (20c). Substituting the Eqs. (22) and (26) in Eq. (A.7) yields,

$$\sigma_{zz}^{(1)}(r,z)=\sum_{m=1}^{\infty}t_m^2\{\lfloor\upsilon_1\cosh(t_mz_1)\alpha_{1m}+\upsilon_2\cosh(t_mz_2)\rfloor B_{2m}+[\upsilon_1\cosh(t_mz_1)\alpha_{2m}+\upsilon_3\cosh(t_mz_3)]B_{3m}\}H_0(t_mr) \tag{30}$$

where

$$H_j(t_mr)=-\frac{Y_1(t_ma)}{J_1(t_ma)}J_j(t_mr)+Y_j(t_mr)\quad(j=0,1) \tag{31}$$

Substitution of Eqs. (28a) and (28b) in Eq. (A.12) yields,

$$\begin{aligned}\sigma_{zz}^{(2)}(r,z)=-\sum_{n=1}^{\infty}s_n^2\Bigg\{&\left[\upsilon_1\lambda_1\frac{\gamma_2(a)\xi_0-\gamma_3(a)}{\gamma_1(a)}I_0(s_nr_1)-\upsilon_2\lambda_2\xi_0I_0(s_nr_2)+\upsilon_3\lambda_3I_0(s_nr_3)\right]G_{3n}\\&+\sum_{i=1}^{3}\left[\upsilon_1\lambda_1\frac{\gamma_2(a)\xi_i+\kappa_i(a)}{\gamma_1(a)}I_0(s_nr_1)-\upsilon_2\lambda_2\xi_iI_0(s_nr_2)+\upsilon_i\lambda_iK_0(s_nr_i)\right]L_{in}\Bigg\}\cos(s_nz)\end{aligned} \tag{32}$$

Next, following an identical procedure, $D_z^{(1)}$ can be expressed as,

$$D_z^{(1)}(r,z)=\sum_{m=1}^{\infty}t_m^2\{[\tau_1\cosh(t_mz_1)\alpha_{1m}+\tau_2\cosh(t_mz_2)]B_{2m}+[\tau_1\cosh(t_mz_1)\alpha_{2m}+\tau_3\cosh(t_mz_3)]B_{3m}\}H_0(t_mr) \tag{33}$$

and

$$\begin{aligned}D_z^{(2)}(r,z)=-\sum_{n=1}^{\infty}s_n^2\Bigg\{&\left[\tau_1\lambda_1\frac{\gamma_2(a)\xi_0-\gamma_3(a)}{\gamma_1(a)}I_0(s_nr_1)-\tau_2\lambda_2\xi_0I_0(s_nr_2)+\tau_3\lambda_3I_0(s_nr_3)\right]G_{3n}\\&+\sum_{i=1}^{3}\left[\tau_1\lambda_1\frac{\gamma_2(a)\xi_i+\kappa_i(a)}{\gamma_1(a)}I_0(s_nr_1)-\tau_2\lambda_2\xi_iI_0(s_nr_2)+\tau_i\lambda_iK_0(s_nr_i)\right]L_{in}\Bigg\}\cos(s_nz)\end{aligned} \tag{34}$$

Substitution of Eqs. (22) and (26) in Eq. (A.9) yields the following expression for $D_r^{(1)}$.

$$D_r^{(1)}(r,z)=\sum_{m=1}^{\infty}\{[\varsigma_1\sinh(t_mz_1)\alpha_{1m}+\varsigma_2\sinh(t_mz_2)]B_{2m}+[\varsigma_1\sinh(t_mz_1)\alpha_{2m}+\varsigma_3\sinh(t_mz_3)]B_{3m}\}H_1(t_mr) \tag{35}$$

Substitution of Eqs. (28a) and (28b) in Eq. (A.14) yields,

$$\begin{aligned}D_r^{(2)}(r,z)=-\sum_{n=1}^{\infty}s_n^2\Bigg\{&\left[\frac{\gamma_2(a)\xi_0-\gamma_3(a)}{\gamma_1(a)}\varpi_1(r)-\xi_0\varpi_2(r)+\varpi_3(r)\right]G_{3n}\\&+\sum_{i=1}^{3}\left[\frac{\gamma_2(a)\xi_i+\kappa_i(a)}{\gamma_1(a)}\varpi_1(r)-\xi_i\varpi_2(r)-\rho_i(r)\right]L_{in}\Bigg\}\sin(s_nz)\end{aligned} \tag{36}$$

where

$$\varpi_i(r)=\varsigma_i\lambda_iI_1(s_nr_i);\quad\rho_i(r)=\varsigma_i\lambda_iK_1(s_nr_i)\quad(i=1,2,3) \tag{37}$$

Following an identical procedure, $\sigma_{rr}^{(1)}$ can be expressed as,

$$\sigma_{rr}^{(1)}(r,z)=\sum_{m=1}^{\infty}t_m\Bigg\{\Big[[\alpha_{1m}\cosh(t_mz_1)+\cosh(t_mz_2)]\Big[-c_{11}t_mH_0(t_mr)+(c_{11}-c_{12})\frac{1}{r}H_1(t_mr)\Big]$$
$$+t_m[\chi_1\alpha_{1m}\cosh(t_mz_1)+\chi_2\cosh(t_mz_2)]H_0(t_mr)\Big]B_{2m}+\Big[[\alpha_{2m}\cosh(t_mz_1)+\cosh(t_mz_3)]$$
$$\times\Big[-c_{11}t_mH_0(t_mr)+(c_{11}-c_{12})\frac{1}{r}H_1(t_mr)\Big]+t_m[\chi_1\alpha_{2m}\cosh(t_mz_1)+\chi_3\cosh(t_mz_3)]H_0(t_mr)\Big]B_{3m}\Bigg\} \tag{38}$$

Using Eqs. (28a), (28b) and (A.11), $\sigma_{rr}^{(2)}$ can be expressed as,

$$\sigma_{rr}^{(2)}(r,z)=\sum_{n=1}^{\infty}\left[\Gamma_{0n}G_{3n}+\sum_{i=1}^{3}\Gamma_{in}L_{in}\right]\cos(s_nz) \tag{39}$$

where $\Gamma_{in}(i=0,1,2,3)$ are defined in the Appendix (Eqs. (A.17) and (A.18)).

All components of stresses and electric displacements involving the remaining boundary conditions are now expressed in terms of the arbitrary functions B_{2m}, B_{3m}, G_{3n} and $L_{in}(i=1,2,3)$. Assuming that the series involving m and n indices converge for M and N terms, the remaining boundary conditions of the cylinder have to be used to determine the $(2M+4N)$ unknown arbitrary functions appearing in the general solution. Until now only the shear stress boundary condition is used and the remaining boundary conditions involving radial and vertical normal stresses and electric displacements can be used to determine the $(2M+4N)$ arbitrary functions.

Now consider the boundary condition $\sigma_{rr}=0$ at $r=a$, which can be expressed as,

$$(\sigma_{rr}^{(1)}+\sigma_{rr}^{(2)}+\sigma_{rr}^{(0)})_{r=a}=0 \tag{40}$$

Noting that $H_1(t_ma)=0$, Eq. (38) is reduced to

$$\sigma_{rr}^{(1)}(a,z)=\sum_{m=1}^{\infty}t_m^2\{[-c_{11}(\alpha_{1m}\cosh(t_mz_1)+\cosh(t_mz_2))+\chi_1\alpha_{1m}\cosh(t_mz_1)+\chi_2\cosh(t_mz_2)]B_{2m}$$
$$+[-c_{11}(\alpha_{2m}\cosh(t_mz_1)+\cosh(t_mz_3))+\chi_1\alpha_{2m}\cosh(t_mz_1)+\chi_3\cosh(t_mz_3)]B_{3m}\}H_0(t_ma) \tag{41}$$

In order to apply the boundary condition given by Eq. (40) at a constant r value, it is necessary to express the variation of radial stress in the z-direction in terms of identical functions of z. To achieve this, the hyperbolic cosine terms in Eq. (41) are expressed in terms of a Fourier series of the following form:

$$\cosh(t_mz_i)=y_0^{(i)}+\sum_{n=1}^{\infty}y_n^{(i)}\cos(s_nz)\quad(i=1,2,3) \tag{42}$$

where

$$y_0^{(i)}=\frac{\sinh(t_mh_i)}{h_it_m};\quad y_n^{(i)}=\frac{2t_m\sinh(t_mh_i)\cos(n\pi)}{h_i(t_m^2+\lambda_is_n^2)} \tag{43}$$

Substitution of Eq. (42) in Eq. (41) makes the z-coordinate dependence of Eqs. (41) and (39) identical and thus allows the grouping of terms with similar cosine functions. Then applying the boundary condition given by Eq. (40) yields the following set of linear relationship between the arbitrary functions.

$$\sum_{i=1}^{3}2(c_{11}+c_{12}-2\chi_i)A_{0i}+(c_{12}-c_{11})\frac{1}{a^2}B_{01}+\sum_{m=1}^{\infty}t_m^2\{[-c_{11}(\alpha_{1m}y_0^{(1)}+y_0^{(2)})+\chi_1\alpha_{1m}y_0^{(1)}+\chi_2y_0^{(2)}]B_{2m}$$
$$+[-c_{11}(\alpha_{2m}y_0^{(1)}+y_0^{(3)})+\chi_1\alpha_{2m}y_0^{(1)}+\chi_3y_0^{(3)}]B_{3m}\}H_0(t_ma)=0 \tag{44a}$$

$$\sum_{m=1}^{\infty} t_m^2 \left\{ \left[-c_{11}\left(\alpha_{1m} y_n^{(1)} + y_n^{(2)}\right) + \chi_1 \alpha_{1m} y_n^{(1)} + \chi_2 y_n^{(2)} \right] B_{2m} \right.$$
$$\left. + \left[-c_{11}\left(\alpha_{2m} y_n^{(1)} + y_n^{(3)}\right) + \chi_1 \alpha_{2m} y_n^{(1)} + \chi_3 y_n^{(3)} \right] B_{3m} \right\} H_0(t_m a) + \Gamma_{0n} G_{3n} + \sum_{i=1}^{3} \Gamma_{in} L_{in} = 0 \tag{44b}$$

Next, it is straightforward to apply the boundary condition $\sigma_{rr} = 0$ at $r = 1$. Noting that $H_1(t_m) = 0$, $\sigma_{rr}^{(1)}$ at $r = 1$ can be obtained simply by replacing 'a' in Eq. (41) by '1'. Then using Eqs. (42), (43) and (39), the following linear relationships between the arbitrary coefficients are obtained.

$$\sum_{i=1}^{3} 2(c_{11} + c_{12} - 2\chi_i) A_{0i} + (c_{12} - c_{11}) B_{01} + \sum_{m=1}^{\infty} t_m^2 \left\{ \left[-c_{11}\left(\alpha_{1m} y_0^{(1)+y_0^{(2)}}\right) + \chi_1 \alpha_{1m} y_0^{(1)} + \chi_2 y_0^{(2)} \right] B_{2m} \right.$$
$$\left. + \left[-c_{11}\left(\alpha_{2m} y_0^{(1)} + y_0^{(3)}\right) + \chi_1 \alpha_{2m} y_0^{(1)} + \chi_3 y_0^{(3)} \right] B_{3m} \right\} H_0(t_m) = 0 \tag{45a}$$

$$\sum_{m=1}^{\infty} t_m^2 \left\{ \left[-c_{11}\left(\alpha_{1m} y_n^{(1)} + y_n^{(2)}\right) + \chi_1 \alpha_{1m} y_n^{(1)} + \chi_2 y_n^{(2)} \right] B_{2m} \right.$$
$$\left. + \left[-c_{11}\left(\alpha_{2m} y_n^{(1)} + y_n^{(3)}\right) + \chi_1 \alpha_{2m} y_n^{(1)} + \chi_3 y_n^{(3)} \right] B_{3m} \right\} H_0(t_m) + \Gamma_{0n} G_{3n} + \sum_{i=1}^{3} \Gamma_{in} L_{in} = 0 \tag{45b}$$

The boundary condition $D_r = 0$ at $r = a, 1$ can be expressed as,

$$\left(D_r^{(1)} + D_r^{(2)} + D_r^{(0)}\right)_{r=a} = 0; \quad \left(D_r^{(1)} + D_r^{(2)} + D_r^{(0)}\right)_{r=1} = 0 \tag{46}$$

Noting that $D_r^{(1)}(a,z) = 0$, $D_r^{(1)}(1,z) = 0$ and $D_r^{(0)} = 0$, Eq. (46) reduces to,

$$D_r^{(2)}(a,z) = 0; \quad D_r^{(2)}(1,z) = 0 \tag{47}$$

Substitution of Eq. (47) in Eq. (36) yields the following set of linear relations between the arbitrary functions

$$\left(\frac{\gamma_2(a)\xi_0 - \gamma_3(a)}{\gamma_1(a)} \varpi_1(a) - \xi_0 \varpi_2(a) + \varpi_3(a) \right) G_{3n} + \sum_{i=1}^{3} \left(\frac{\gamma_2(a)\xi_i + \kappa_i(a)}{\gamma_1(a)} \varpi_1(a) - \xi_i \varpi_2(a) - \rho_i(a) \right) L_{in} = 0 \tag{48a}$$

$$\left(\frac{\gamma_2(a)\xi_0 - \gamma_3(a)}{\gamma_1(a)} \varpi_1(1) - \xi_0 \varpi_2(1) + \varpi_3(1) \right) G_{3n} + \sum_{i=1}^{3} \left(\frac{\gamma_2(a)\xi_i + \kappa_i(a)}{\gamma_1(a)} \varpi_1(1) - \xi_i \varpi_2(1) - \rho_i(1) \right) L_{in} = 0 \tag{48b}$$

Next, consider the boundary condition $\sigma_{zz} = -p(r)$ at $z = \pm h$ which can be expressed as,

$$\left(\sigma_{zz}^{(1)} + \sigma_{zz}^{(2)} + \sigma_{zz}^{(0)}\right)_{z=\pm h} = -p(r) \tag{49}$$

In order to apply Eq. (49), it is necessary to transform each term of Eq. (49) to identical functional variations of the radial coordinate. To achieve this, first expand $p(r)$ into a Fourier–Bessel series of the following form.

$$p(r) = P_0 + \sum_{m=1}^{\infty} P_m H_0(t_m r) \tag{50}$$

where

$$P_0 = \frac{2\int_a^1 p(r) r\,\mathrm{d}r}{1-a^2}; \quad P_m = \frac{\int_a^1 p(r) r H_0(t_m r)\,\mathrm{d}r}{\int_a^1 r H_0^2(t_m r)\,\mathrm{d}r} \tag{51}$$

Then express the Bessel and the modified Bessel functions of the second kind, i.e. $I_0(s_n r_i)$ and $K_0(s_n r_i)(i=1,2,3)$, in Eq. (32) in terms of Fourier–Bessel series as,

$$I_0(s_n r_i) = l_0^{(i)} + \sum_{m=1}^{\infty} l_m^{(i)} H_0(t_m r); \quad K_0(s_n r_i) = \delta_0^{(i)} + \sum_{m=1}^{\infty} \delta_m^{(i)} H_0(t_m r) \quad (i=1,2,3) \tag{52}$$

where

$$l_0^{(i)} = -\frac{-I_1(\sqrt{\lambda_i} s_n) + a I_1(\sqrt{\lambda_i} s_n a)}{\sqrt{\lambda_i} s_n} \frac{2}{1-a^2}; \quad l_m^{(i)} = \frac{\int_a^1 I_0(s_n r_i) r H_0(t_m r)\,\mathrm{d}r}{\int_a^1 r H_0^2(t_m r)\,\mathrm{d}r} \tag{53a}$$

$$\delta_0^{(i)} = \frac{-K_1(\sqrt{\lambda_i} s_n) + a K_1(\sqrt{\lambda_i} s_n a)}{\sqrt{\lambda_i} s_n} \frac{2}{1-a^2}; \quad \delta_m^{(i)} = \frac{\int_a^1 K_0(s_n r_i) r H_0(t_m r)\,\mathrm{d}r}{\int_a^1 r H_0^2(t_m r)\,\mathrm{d}r} \tag{53b}$$

Substitution of Eqs. (A.4), (30), (32), (50) and (52) in Eq. (49) yields the following linear relationships between the arbitrary coefficients.

$$4\sum_{i=1}^{3} \upsilon_i A_{0i} + \sum_{i=1}^{3} \upsilon_i \lambda_i \sum_{n=1}^{\infty} s_n^2 (l_0^{(i)} G_{in} + \delta_0^{(i)} L_{in}) \cos(n\pi) = P_0 \tag{54a}$$

$$\begin{aligned} & t_m^2 \{[\upsilon_1 \alpha_{1m} \cosh(t_m h_1) + \upsilon_2 \cosh(t_m h_2)] B_{2m} + [\upsilon_1 \alpha_{2m} \cosh(t_m h_1) + \upsilon_3 \cosh(t_m h_3)] B_{3m}\} \\ & - \sum_{n=1}^{\infty} s_n^2 \left[\left(\upsilon_1 \lambda_1 l_m^{(1)} \frac{\gamma_2(a)\xi_0 - \gamma_3(a)}{\gamma_1(a)} - \upsilon_2 \lambda_2 l_m^{(2)} \xi_0 + \upsilon_3 \lambda_3 l_m^{(3)} \right) G_{3n} \right. \\ & \left. + \sum_{i=1}^{3} \left(\upsilon_1 \lambda_1 l_m^{(1)} \frac{\gamma_2(a)\xi_i + \kappa_i(a)}{\gamma_1(a)} - \upsilon_2 \lambda_2 l_m^{(2)} \xi_i + \upsilon_i \lambda_i \delta_m^{(i)} \right) L_{in} \right] \cos(n\pi) = -P_m \end{aligned} \tag{54b}$$

Finally, the remaining boundary condition $D_z = 0$ at $z = \pm h$ can be expressed as,

$$\left(D_z^{(1)} + D_z^{(2)} + D_z^{(0)}\right)_{z=\pm h} = 0 \tag{55}$$

Substitution of Eqs. (A.5), (33), (34) and (52) in Eq. (55) yields the following linear relationships between the arbitrary coefficients.

$$4\sum_{i=1}^{3} \tau_i A_{0i} + \sum_{i=1}^{3} \tau_i \lambda_i \sum_{n=1}^{\infty} s_n^2 (l_0^{(i)} G_{in} + \delta_0^{(i)} L_{in}) \cos(n\pi) = 0 \tag{56a}$$

$$\begin{aligned} & t_m^2 \{[\tau_1 \alpha_{1m} \cosh(t_m h_1) + \tau_2 \cosh(t_m h_2)] B_{2m} + [\tau_1 \alpha_{2m} \cosh(t_m h_1) + \tau_3 \cosh(t_m h_3)] B_{3m}\} \\ & - \sum_{n=1}^{\infty} s_n^2 \left[\left(\tau_1 \lambda_1 l_m^{(1)} \frac{\gamma_2(a)\xi_0 - \gamma_3(a)}{\gamma_1(a)} - \tau_2 \lambda_2 l_m^{(2)} \xi_0 + \tau_3 \lambda_3 l_m^{(3)} \right) G_{3n} \right. \\ & \left. + \sum_{i=1}^{3} \left(\tau_1 \lambda_1 l_m^{(1)} \frac{\gamma_2(a)\xi_i + \kappa_i(a)}{\gamma_1(a)} - \tau_2 \lambda_2 l_m^{(2)} \xi_i + \tau_i \lambda_i \delta_m^{(i)} \right) L_{in} \right] \cos(n\pi) = 0 \end{aligned} \tag{56b}$$

The Eqs. (44b), (45b), (48a), (48b), (54b) and (56b) constitute a system of linear algebraic equations of order $(2M + 4N)$ with arbitrary constants $B_{2m}, B_{3m}, G_{3n}, L_{1n}, L_{2n}$ and L_{3n} . This system can be solved numerically. In addition, Eqs. (44a), (45a), (54a) and (56a) can be solved for the remaining four arbitrary constants $A_{0i}(i = 1, 2, 3)$ and B_{01}. This completes the solution of all arbitrary coefficients appearing in the general solution for the vertical loading case shown in Fig. 1.

3.1. Electric charge loading case

Now consider the case of a cylinder where electric charge loading of uniform intensity is applied to the top and bottom surfaces over an annular ring of inner and outer radii equal to a and b_0 respectively. The boundary conditions can be expressed as follows,

$$\sigma_{rr}(a,z) = 0, \quad \sigma_{rz}(a,z) = 0, \quad D_r(a,z) = 0 \quad \text{for} \quad -h \leqslant z \leqslant h \tag{57a}$$

$$\sigma_{rr}(1,z) = 0, \quad \sigma_{rz}(1,z) = 0, \quad D_r(1,z) = 0 \quad \text{for} \quad -h \leqslant z \leqslant h \tag{57b}$$

$$\sigma_{zz}(r,\pm h) = 0, \quad \sigma_{zr}(r,\pm h) = 0, \quad D_z(r,\pm h) = -q(r) \quad \text{for } a \leqslant r \leqslant 1 \tag{57c}$$

where $q(r)$ denotes the nondimensional magnitude of electric charge applied to the top and bottom surfaces of the cylinder.

The solution of this problem is quite similar to that of a cylinder subjected to vertical pressure on top and bottom surfaces. The only difference is for $z = \pm h$, the vertical stress σ_{zz} is equal to zero for $a \leqslant r \leqslant 1$ while the vertical electric displacement is equal to $-q(r)$ for $a \leqslant r \leqslant 1$. Therefore, the Eqs. (54a) and (54b) are changed to,

$$4\sum_{i=1}^{3} \upsilon_i A_{0i} + \sum_{i=1}^{3} \upsilon_i \lambda_i \sum_{n=1}^{\infty} s_n^2 \left(l_0^{(i)} G_{in} + \delta_0^{(i)} L_{in} \right) \cos(n\pi) = 0 \tag{58a}$$

$$\begin{aligned} & t_m^2 \{ [\upsilon_1 \alpha_{1m} \cosh(t_m h_1) + \upsilon_2 \cosh(t_m h_2)] B_{2m} + [\upsilon_1 \alpha_{2m} \cosh(t_m h_1) + \upsilon_3 \cosh(t_m h_3)] B_{3m} \} \\ & \quad - \sum_{n=1}^{\infty} s_n^2 \left[\left(\upsilon_1 \lambda_1 l_m^{(1)} \frac{\gamma_2(a)\xi_0 - \gamma_3(a)}{\gamma_1(a)} - \upsilon_2 \lambda_2 l_m^{(2)} \xi_0 + \upsilon_3 \lambda_3 l_m^{(3)} \right) G_{3n} \right. \\ & \quad \left. + \sum_{i=1}^{3} \left(\upsilon_1 \lambda_1 l_m^{(1)} \frac{\gamma_2(a)\xi_i + \kappa_i(a)}{\gamma_1(a)} - \upsilon_2 \lambda_2 l_m^{(2)} \xi_i + \upsilon_i \lambda_i \delta_m^{(i)} \right) L_{in} \right] \cos(n\pi) = 0 \end{aligned} \tag{58b}$$

Expand $q(r)$ into a Fourier–Bessel series of the following form,

$$q(r) = Q_0 + \sum_{m=1}^{\infty} Q_m H_0(t_m r) \tag{59}$$

where

$$Q_0 = \frac{2\int_a^1 q(r) r \, \mathrm{d}r}{1 - a^2}; \quad Q_m = \frac{\int_a^1 q(r) r H_0(t_m r) \, \mathrm{d}r}{\int_a^1 r H_0^2(t_m r) \, \mathrm{d}r} \tag{60}$$

Therefore, the Eqs. (56a) and (56b) are changed to,

$$4\sum_{i=1}^{3} \tau_i A_{0i} + \sum_{i=1}^{3} \tau_i \lambda_i \sum_{n=1}^{\infty} s_n^2 (l_0^{(i)} G_{in} + \delta_0^{(i)} L_{in}) \cos(n\pi) = Q_0 \tag{61a}$$

$$t_m^2\{[\tau_1\alpha_{1m}\cosh(t_m h_1)+\tau_2\cosh(t_m h_2)]B_{2m}+[\tau_1\alpha_{2m}\cosh(t_m h_1)+\tau_3\cosh(t_m h_3)]B_{3m}\}$$
$$-\sum_{n=1}^{\infty}s_n^2\left[\left(\tau_1\lambda_1 l_m^{(1)}\frac{\gamma_2(a)\xi_0-\gamma_3(a)}{\gamma_1(a)}-\tau_2\lambda_2 l_m^{(2)}\xi_0+\tau_3\lambda_3 l_m^{(3)}\right)G_{3n}\right.$$
$$\left.+\sum_{i=1}^{3}\left(\tau_1\lambda_1 l_m^{(1)}\frac{\gamma_2(a)\xi_i+\kappa_i(a)}{\gamma_1(a)}-\tau_2\lambda_2 l_m^{(2)}\xi_i+\tau_i\lambda_i\delta_m^{(i)}\right)L_{in}\right]\cos(n\pi)=-Q_m \tag{61b}$$

Eqs. (44b), (45b), (48a), (48b), (58b) and (61b) constitute a system of linear algebraic equations of order $(2M+4N)$ with the arbitrary constants $B_{2m}, B_{3m}, G_{3n}, L_{1n}, L_{2n}$ and L_{3n}. These equations can be solved numerically. In addition, Eqs. (44a), (45a), (58a) and (61a) can be solved for the remaining four arbitrary constants $A_{0i}(i=1,2,3)$ and B_{01}. This completes the solution of all arbitrary coefficients appearing in the general solution for the electric charge loading case.

4. Numerical results and discussion

4.1. Comparison with elastic cylinders

Numerical stability of the present solution is first investigated by studying the convergence with respect to the total number of terms used in the series expansion (N, M). The overall solution scheme is found to be stable and convergent for a wide range of M and N values. The details of the convergence study are not presented here for brevity and the values of M and N corresponding to each set of numerical results presented in this paper are given separately. Okumura (1989) analyzed the case of a transversely isotropic elastic hollow cylinder subjected to an outer band of load by using analytical techniques. The geometry of the hollow cylinder is such that $b/a=4$, $b/h=1$ and $d/h=0.3$ where 'h' denotes the half-width of the band load. A magnesium cylinder $[c_{11}=5.64, c_{12}=2.30, c_{13}=1.81, c_{33}=5.86, c_{44}=1.68(\times 10^{10}\,\mathrm{N\,m^{-2}})]$ was used in the numerical study. The boundary conditions used by Okumura (1989) are:

$$\sigma_{rr}=0,\quad \sigma_{rz}=0,\quad \text{at } r=a \tag{62a}$$

$$\sigma_{rr}=\begin{cases}-p_0 & |z|\leqslant d\\ 0 & |z|>d\end{cases},\quad \sigma_{rz}=0,\quad \text{at } r=b \tag{62b}$$

$$\sigma_{zz}=0,\quad \sigma_{zr}=0,\quad \text{at } z=\pm h \tag{62c}$$

The present general solution can be used to analyze the boundary-value problem considered by Okumura (1989) by setting the piezoelectric coefficients to negligibly small values ($e_{ij}\approx 0$). Numerical solutions for elastic hollow cylinders are found to converge for $M=11$ and $N=11$ for the loading conditions considered by Okumura (1989). Fig. 2 shows a comparison of the current results with those obtained by Okumura. The two solutions agree very closely. Note that vertical stress at $z^*=z/h=1.0$ has to be equal to zero because of the boundary condition but both solutions (present and Okamura's) are not exactly equal to zero at these locations due to minor precision errors associated with the series solution.

4.2. Response of piezoelectric annular cylinder

4.2.1. Vertical pressure loading

Consider an annular cylinder subjected to a uniform vertical pressure ring load of intensity p_0 over the top and bottom surfaces (Fig. 1). The boundary conditions are expressed as,

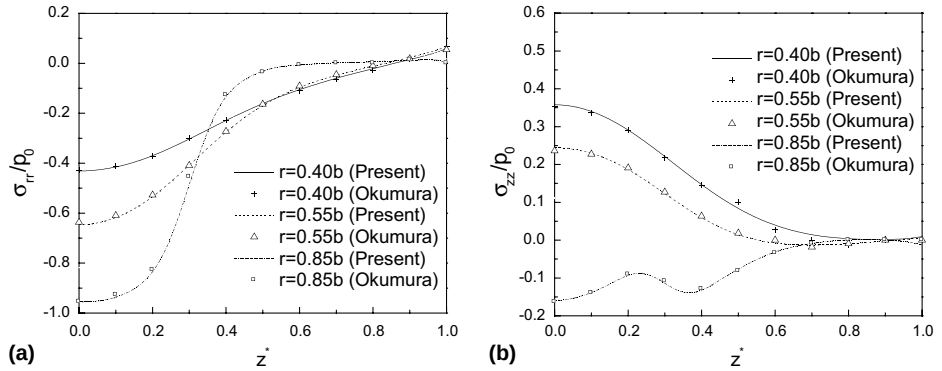

Fig. 2. Comparison of stresses along the z-axis of a hollow magnesium cylinder. (a) Nondimensional radial stress and (b) nondimensional vertical stress.

$$\sigma_{rr} = 0, \quad \sigma_{rz} = 0, \quad D_r = 0, \quad \text{at } r = a \tag{63a}$$

$$\sigma_{rr} = 0, \quad \sigma_{rz} = 0, \quad D_r = 0, \quad \text{at } r = b \tag{63b}$$

$$\sigma_{zz} = \begin{cases} -p_0 & a \leqslant r \leqslant b_0 \\ 0 & b_0 \leqslant r \leqslant b \end{cases}, \quad \sigma_{zr} = 0, \quad D_z = 0, \quad \text{at } z = \pm h \tag{63c}$$

In the numerical study, b_0/b is set to 0.85 and different ratios of h/b (i.e. 0.5, 1.0, 2.0) and a/b (i.e. 0.3, 0.4, 0.5) are considered. The material of the cylinder is PZT-5H [$c_{11} = 12.6, c_{12} = 7.95, c_{13} = 8.41, c_{33} = 11.7, c_{44} = 2.3$ ($\times 10^{10}\,\mathrm{N\,m^{-2}}$); $e_{15} = 17.0, e_{31} = -6.55, e_{33} = 23.3\,(\mathrm{C\,m^{-2}})$; $\varepsilon_{11} = 15.38, \varepsilon_{33} = 12.76\,(\times 10^{-9}\,\mathrm{F\,m^{-1}})$]. The roots $\lambda_i\,(i = 1, 2, 3)$ of Eq. (10) for PZT-5H are $\lambda_1 = 0.82965, \lambda_2 = 0.65573 + 0.70611i$ and $\lambda_3 = 0.65573 - 0.70611i$. Fig. 3 shows the nondimensional vertical stress, $\sigma^*_{zz} = \sigma_{zz}/p_0$, of a cylinder ($h/b = 1$) along the vertical direction ($z^* = z/b$) at $r^* = 0.7$ ($r^* = r/b$) and along the radial direction at $z = 0$ and $z/h = 0.5$ for different a/b ratios. Vertical stress remains compressive along the length and its magnitude decreases rapidly near the loaded end. The magnitude of compressive vertical stress in the middle part of the cylinder decreases slowly with decreasing thickness (increasing a/b ratio) and is nearly constant in the middle of the cylinder for thick

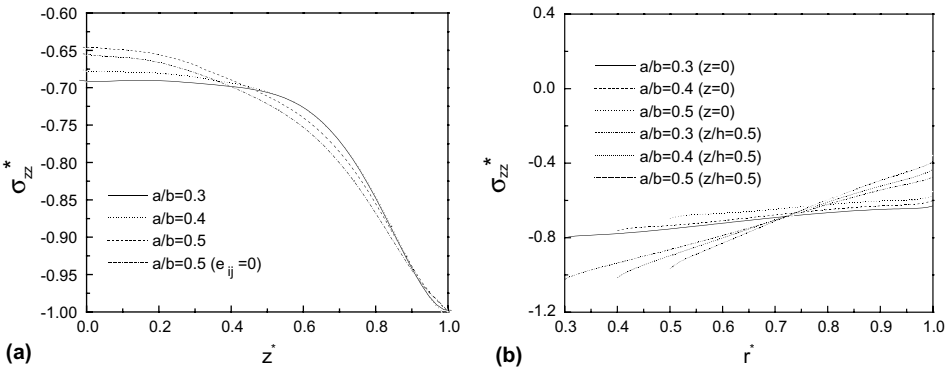

Fig. 3. Vertical stress profiles of a PZT-5H annular cylinder under vertical loading ($b_0/b = 0.85, h/b = 1.0, M = N = 15$). (a) Nondimensional vertical stress along the z-axis at $r = 0.7b$ and (b) nondimensional vertical stress along the r-axis at $z = 0$ and $z/b = 0.5$.

cylinders ($a/b \leqslant 0.3$). Fig. 3(a) also shows the results for a cylinder with no piezoelectric coupling for the case $a/b = 0.5$ and vertical stress of a piezoelectric cylinder is nearly identical (slightly smaller) to that of a non-piezoelectric cylinder.

Fig. 3(b) shows the variation of vertical stress across the thickness of the cylinder at $z/b = 0$ and 0.5. Vertical stress decreases rapidly across the thickness at $z/b = 0.5$ when compared to the mid-plane ($z = 0$). The variation of vertical stress across the thickness is more gradual at the mid-plane and stress at the inner surface is generally higher than that at the outer surface. This is probably a consequence of the loading configuration. The vertical stress profiles corresponding to different wall thicknesses are nearly parallel to each other at the mid-plane and a slight decrease in magnitude is noted with decreasing wall thickness. If the stress state in the mid-plane is equal to the one-dimensional state corresponding to a long cylinder then the stress profiles in Fig. 3(b) would be parallel to the r-axis and the magnitude equal to 0.69, 0.67 and 0.63 for $a/b = 0.3$, 0.4 and 0.5 respectively. The stress state of the cylinder is therefore three-dimensional. The magnitude of vertical stress at the outer surface slightly decreases with decreasing wall thickness.

Fig. 4(a) shows the nondimensional vertical electric displacement, $D_z^* = D_z c_{44}/e_{31}p_0$, at $r^* = 0.7$ due to the vertical loading applied to the ends. D_z^* is zero at the top end (boundary condition) and initially increases rapidly with depth reaching its maximum value near $z/b = 0.9$ for the different cylinder wall thicknesses considered in the present study. The peak value of D_z^* increases as the thickness of the cylinder decreases. At the mid-plane of the cylinder D_z^* is relatively small when compared to its maximum value and the magnitude increases with decreasing cylinder thickness. Fig. 4(b) shows the variation of nondimensional vertical electric field, $E_z^* = E_z e_{31}/p_0$, at $r^* = 0.7$. E_z^* is negative along the length and decreases with decreasing cylinder thickness. Negative vertical electric field has its minimum magnitude at the cylinder ends, increases rapidly with depth near the ends and thereafter becomes nearly constant with depth. It is noted that the electric field in the middle of the cylinder is about 8% higher than the one-dimensional value obtained from the field equations. Note that 1-D solution for vertical electric field can be obtained by inverting Eq. (1) numerically for PZT-5H and then using the 1-D stress field (only nonzero vertical stress) to obtain the corresponding vertical electric field. It is found that 1-D solution for E_z^* is equal to -0.0812. The results in Fig. 4 show the direct piezoelectric effect and represent the typical quasi-static electric response of a short annular cylinder when used as a sensor.

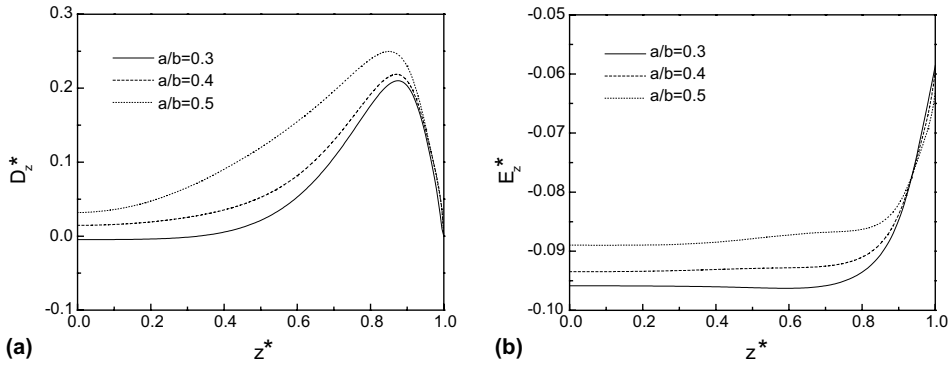

Fig. 4. Vertical electric displacement and vertical electric field of a PZT-5H cylinder under vertical loading ($b_0/b = 0.85$, $h/b = 1.0, M = N = 15$). (a) Nondimensional vertical electric displacement along the z-axis at $r = 0.7b$. (b) Nondimensional vertical electric field along the z-axis at $r = 0.7b$.

4.3. Electric charge loading

Consider an annular cylinder subjected to uniform electric charge density q_0 on the top and bottom surfaces. The boundary conditions can be expressed by Eqs. (63a), (63b) and

$$D_z = \begin{cases} -q_0 & a \leqslant r \leqslant b_0 \\ 0 & b_0 \leqslant r \leqslant b \end{cases}, \quad \sigma_{zz} = 0, \quad \sigma_{zr} = 0, \quad \text{at } z = \pm h \tag{64}$$

Fig. 5(a) and (b) shows the variation of nondimensional vertical electric displacement, $D_z^* = D_z/q_0$, along the vertical and radial directions respectively. Nondimensional vertical electric displacement has a unit magnitude at (boundary condition) and decreases rapidly near the top end. It is nearly constant within the middle half of the cylinder and the magnitude increases slightly with increasing thickness of the cylinder. Fig. 5(b) shows that D_z^* is constant and approaches the 1-D solution in the mid-plane of the cylinder for the three wall thicknesses considered in the present study, i.e. $D_z^* = 0.70$, 0.67 and 0.63 for $a/b = 0.3$, 0.4 and 0.5 respectively. However, at $z/b = 0.5$, the radial variation of D_z^* across the cylinder wall is nonuniform with a higher magnitude at the inner surface. It is noted that the variation of D_z^* in the z- and r-directions is quite similar to that observed for vertical stress under applied vertical pressure.

Fig. 6 shows the nondimensional vertical displacement, $u_z^* = u_z e_{31}/bD_0$, along the z-axis at $r = 0.7b$ for different a/b ratios. Vertical displacement increases linearly along the z-axis (similar to an elastic cylinder under tension) and reaches its maximum value at the ends of the cylinder. u_z^* is only slightly increased with increasing cylinder thickness and this implies that the wall thickness of an annular actuator has a minor influence on the stroke. Fig. 6 shows the converse piezoelectric effect of the cylinder associated with electric loading. In more practical situations, the actuator has a mechanical bias load and is driven by a voltage applied to circular electrodes placed at the cylinder ends. This case involves complex mixed-boundary conditions that require a new formulation of the problem. However, the general solutions given by Eq. (19) can be used to formulate this mixed boundary-value problem.

Fig. 7(a) shows the variation of nondimensional vertical stress, $\sigma_{zz}^* = \sigma_{zz} e_{31}/c_{44} q_0$, in the z-direction at $r^* = 0.7$ for three different values of a/b. Vertical stress is zero at the loading surface due to the boundary condition and is generally compressive inside the cylinder. It increases rapidly near the ends reaching a maximum value in the vicinity of $z^* = z/b = 0.8$. Thereafter, vertical stress decreases rapidly with depth. The magnitude of vertical stress increases with decreasing thickness of the annular cylinder. Fig. 7(b) shows the variation of nondimensional vertical electric field, $E_z^* = E_z e_{31}^2/c_{44} q_0$, in the z-direction at $r^* = 0.7$ and

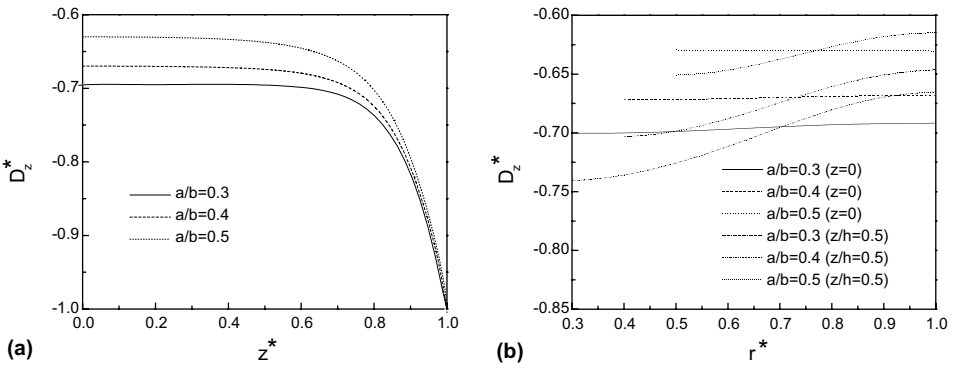

Fig. 5. Vertical electric displacement of a PZT-5H annular cylinder under electric charge loading ($b_0/b = 0.85, h/b = 1.0, M = N = 15$). (a) Nondimensional vertical electric displacement along the z-axis at $r = 0.7b$ and (b) nondimensional vertical electric displacement along the r-axis at $z = 0$ and $z/h = 0.5$.

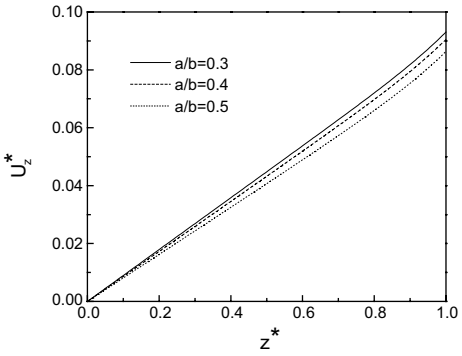

Fig. 6. Nondimensional vertical displacement along the z-axis at $r = 0.7b$ of a PZT-5H annular cylinder under electric charge loading ($b_0/b = 0.85, h/b = 1.0, M = N = 15$).

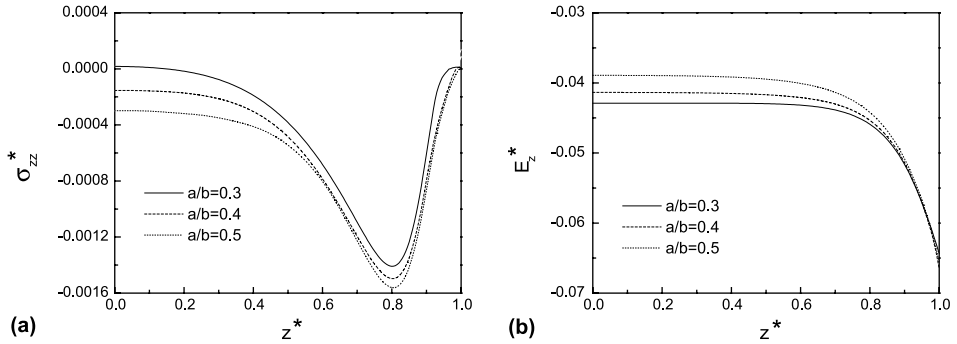

Fig. 7. Vertical stress and electric field of a PZT-5H annular cylinder under electric charge loading ($b_0/b = 0.85$, $h/b = 1.0, M = N = 15$). (a) Nondimensional vertical stress along the z-axis at $r = 0.7b$ and (b) nondimensional vertical electric field along the z-axis at $r = 0.7b$.

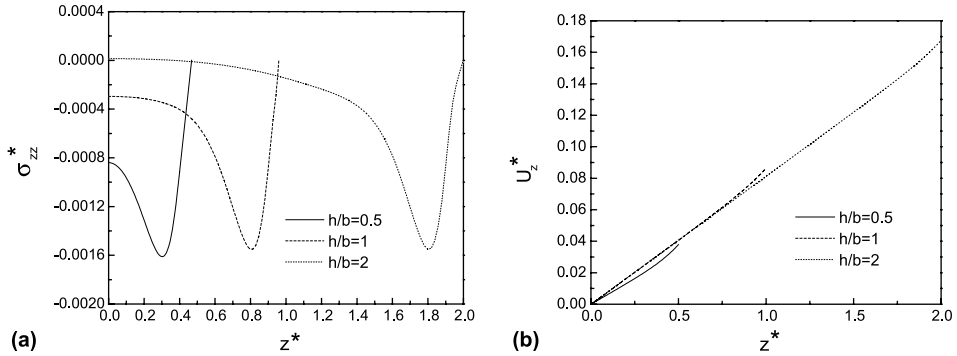

Fig. 8. Vertical stress and displacement along the z-axis at $r = 0.7b$ of a PZT-5H annular cylinder under electric charge loading ($b_0/b = 0.85, a/b = 0.5$). (a) Nondimensional vertical stress profiles along the z-axis at $r = 0.7b$ and (b) nondimensional vertical displacement profiles along the z-axis at $r = 0.7b$.

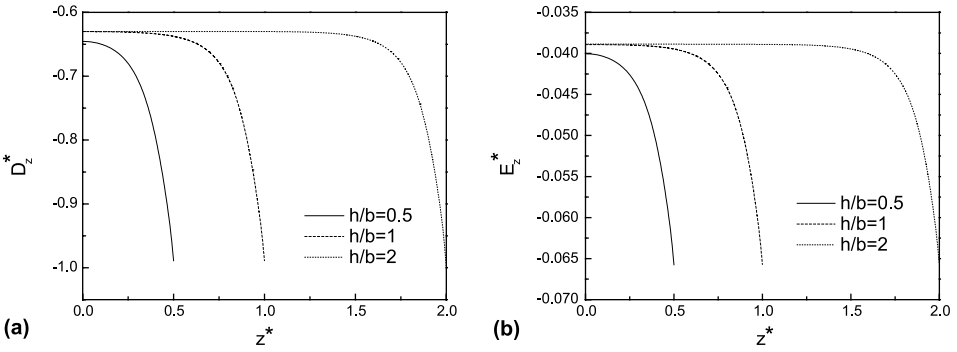

Fig. 9. Vertical electric displacement and vertical electric field of a PZT-5H annular cylinder under electric charge loading ($b_0/b = 0.85, a/b = 0.5$). (a) Nondimensional vertical electric displacement profiles along the z-axis at $r = 0.7b$ and (b) nondimensional vertical electric field profiles along the z-axis at $r = 0.7b$.

the behaviour is very similar to that of D_z^*. The distribution of vertical stress and vertical electric field at the mid-plane of the cylinder was also considered. It is found that σ_{zz}^* and E_z^* are nearly constant at the mid-plane if $h/b \geqslant 1$ and are nonuniform for shorter cylinders ($h/b < 1$) with peak values usually occurring near or at the inside surface of the cylinder.

Figs. 8 and 9 show the variation of nondimensional vertical stress, vertical displacement, vertical electric displacement and vertical electric field at $r^* = 0.7$ for different cylinder lengths (h/b ratios). The solution converges for $M = 15$ and $N = 15$ when $h/b \leqslant 1$, and for $M = 30$ and $N = 30$ when $h/b = 2$. Vertical stress is zero at the top surface due to the boundary condition. It is compressive and increases rapidly with depth near the top surface and reduces to a negligible value in the middle of the cylinder for $h/b > 1$. Fig. 8(b) implies that the average strain in the cylinder is nearly equal for the three different heights so the maximum value of nondimensional vertical displacement is directly proportional to the length-radius ratio of the cylinder. Fig. 9 indicates that both of D_z^*, and E_z^* decay rapidly with depth from the loaded end and approach the 1-D solution for a long cylinder in the middle part of the cylinder when $h/b \geqslant 2$.

5. Conclusions

A generalized displacement potential function method together with a Fourier–Bessel series expansion is successfully used to obtain the exact analytical general solution for fully coupled electroelastic field of an annular piezoelectric cylinder of finite length subjected to axi-symmetric loading. The series solution shows good numerical stability and convergence. Numerical solutions for stresses obtained from the present study agree very closely with the existing solutions for the limiting case of an elastic cylinder. In the case of long cylinders ($h/b \geqslant 2$) subjected to vertical end loads or end electric charge, vertical stress, vertical electric displacement and vertical electric field are uniform in the middle part of the cylinder and are very close to the one-dimensional solution. Both vertical electric displacement and electric field have their maximum values near the loading surface under applied vertical pressure. Similarly, vertical stress is compressive and maximum near the cylinder ends under electric charge loading applied to the ends. Electroelastic field of a short cylinder ($h/b \leqslant 1$) is three-dimensional and shows complex dependence on geometry and material properties. The general solution derived in this paper can be used to analyze a variety of problems such as the effective properties of a unit cell of a 1–3 piezocomposite, fracture mechanics of cylindrical actuators and piezocomposites and other mixed boundary-value problems involving annular actuators and resonators.

Acknowledgement

The work presented in this paper was supported by a research grant from the Natural Sciences and Engineering Research Council of Canada.

Appendix A

The constants $\Omega_i (i = 1,2,3,4)$ appearing in Eq. (10) are defined by,

$$\begin{aligned}
\Omega_1 &= e_{15}^2 c_{11} + \overline{\varepsilon}_{11} c_{11} \\
\Omega_2 &= \overline{\varepsilon}_{11} c_{13}^2 + 2e_{15}^2 c_{13} + 2\overline{\varepsilon}_{11} c_{13} + 2e_{15} c_{13} - 1 - 2e_{33} e_{15} c_{11} - \overline{\varepsilon}_{33} c_{11} - \overline{\varepsilon}_{11} c_{33} c_{11} \\
\Omega_3 &= -\overline{\varepsilon}_{33} c_{13}^2 - 2e_{15} e_{33} c_{13} - 2e_{33} c_{13} - 2\overline{\varepsilon}_{33} c_{13} - 2e_{33} + e_{33}^2 c_{11} + 2e_{15} c_{33} + e_{15}^2 c_{33} + \overline{\varepsilon}_{33} c_{33} c_{11} + \overline{\varepsilon}_{11} c_{33} + c_{33} \\
\Omega_4 &= -e_{33}^2 - \overline{\varepsilon}_{33} c_{33}
\end{aligned} \tag{A.1}$$

The solution for $\overline{\psi}$ has the following form depending on the nature of the roots $\lambda_i (i = 1,2,3)$.

$$\begin{aligned}
&\overline{\psi} = \overline{\psi}_1 + \overline{\psi}_2 + \overline{\psi}_3 \qquad \text{for } \lambda_1 \neq \lambda_2 \neq \lambda_3 \\
&\overline{\psi} = \overline{\psi}_1 + \overline{\psi}_2 + \mathbf{z}\overline{\psi}_3 \qquad \text{for } \lambda_1 \neq \lambda_2 = \lambda_3 \\
&\overline{\psi} = \overline{\psi}_1 + \mathbf{z}\overline{\psi}_2 + \mathbf{z}^2\overline{\psi}_3 \quad \text{for } \lambda_1 = \lambda_2 = \lambda_3
\end{aligned} \tag{A.2}$$

The solutions for stresses and electric displacements corresponding to Eq. (19) can be expressed as,

$$\sigma_{rr}^{(0)}(r) = (c_{12} - c_{11})\frac{1}{r^2} B_{01} + \sum_{i=1}^{3} 2(c_{11} + c_{12} - 2\chi_i) A_{0i} \tag{A.3}$$

$$\sigma_{zz}^{(0)} = -4\sum_{i=1}^{3} \upsilon_i A_{0i}; \quad \sigma_{zr}^{(0)} = 0 \tag{A.4}$$

$$D_z^{(0)} = -4\sum_{i=1}^{3} \tau_i A_{0i}; \quad D_r^{(0)} = 0 \tag{A.5}$$

$$\begin{aligned}
\sigma_{rr}^{(1)}(r,z) = \sum_{i=1}^{3}\sum_{m=1}^{\infty} t_m \Bigg\{ &\left[(-c_{11} + \chi_i) t_m J_0(t_m r) + (c_{11} - c_{12})\frac{1}{r} J_1(t_m r)\right] A_{im} \\
&+ \left[(-c_{11} + \chi_i) t_m Y_0(t_m r) + (c_{11} - c_{12})\frac{1}{r} Y_1(t_m r)\right] B_{im} \Bigg\} \cosh(t_m z_i)
\end{aligned} \tag{A.6}$$

$$\sigma_{zz}^{(1)}(r,z) = \sum_{i=1}^{3} \upsilon_i \sum_{m=1}^{\infty} t_m^2 [A_{im} J_0(t_m r) + B_{im} Y_0(t_m r)] \cosh(t_m z_i) \tag{A.7}$$

$$\sigma_{zr}^{(1)}(r,z) = -\sum_{i=1}^{3} \vartheta_i \sum_{m=1}^{\infty} t_m^2 [A_{im} J_1(t_m r) + B_{im} Y_1(t_m r)] \sinh(t_m z_i) \tag{A.8}$$

$$D_r^{(1)}(r,z) = -\sum_{i=1}^{3} \varsigma_i \sum_{m=1}^{\infty} t_m^2 [A_{im} J_1(t_m r) + B_{im} Y_1(t_m r)] \sinh(t_m z_i) \tag{A.9}$$

$$D_z^{(1)}(r,z) = \sum_{i=1}^{3} \tau_i \sum_{m=1}^{\infty} t_m^2 [A_{im} J_0(t_m r) + B_{im} Y_0(t_m r)] \cosh(t_m z_i) \tag{A.10}$$

$$\begin{aligned}\sigma_{rr}^{(2)}(r,z) = \sum_{i=1}^{3} \sum_{n=1}^{\infty} \sqrt{\lambda_i} s_n \Bigg\{ &\left[(c_{11} - \chi_i) \sqrt{\lambda_i} s_n I_0(s_n r_i) + (c_{12} - c_{11}) \frac{1}{r} I_1(s_n r_i) \right] G_{in} \\ &+ \left[(c_{11} + \chi_i) \sqrt{\lambda_i} s_n K_0(s_n r_i) - (c_{12} - c_{11}) \frac{1}{r} K_1(s_n r_i) \right] L_{in} \Bigg\} \cos(s_n z)\end{aligned} \tag{A.11}$$

$$\sigma_{zz}^{(2)}(r,z) = -\sum_{i=1}^{3} \upsilon_i \sum_{n=1}^{\infty} \lambda_i s_n^2 [G_{in} I_0(s_n r_i) + L_{in} K_0(s_n r_i)] \cos(s_n z) \tag{A.12}$$

$$\sigma_{zr}^{(2)}(r,z) = -\sum_{i=1}^{3} \vartheta_i \sum_{n=1}^{\infty} \lambda_i s_n^2 [G_{in} I_1(s_n r_i) - L_{in} K_1(s_n r_i)] \sin(s_n z) \tag{A.13}$$

$$D_r^{(2)}(r,z) = -\sum_{i=1}^{3} \varsigma_i \sum_{n=1}^{\infty} \lambda_i s_n^2 [G_{in} I_1(s_n r_i) - L_{in} K_1(s_n r_i)] \sin(s_n z) \tag{A.14}$$

$$D_z^{(2)}(r,z) = -\sum_{i=1}^{3} \tau_i \sum_{n=1}^{\infty} \lambda_i s_n^2 [G_{in} I_0(s_n r_i) + L_{in} K_0(s_n r_i)] \cos(s_n z) \tag{A.15}$$

where

$$\begin{aligned}&\chi_i = (c_{13} k_{1i} + k_{2i})/\lambda_i; \quad \upsilon_i = (c_{33} k_{1i} + e_{33} k_{2i})/\lambda_i - c_{13}; \quad \vartheta_i = (1 + k_{1i} + e_{15} k_{2i})/\sqrt{\lambda_i} \\ &\varsigma_i = (e_{15} + e_{15} k_{1i} - \overline{\varepsilon}_{11} k_{2i})/\sqrt{\lambda_i}; \quad \tau_i = (e_{33} k_{1i} - \overline{\varepsilon}_{33} k_{2i})/\lambda_i - 1 \quad (i = 1,2,3)\end{aligned} \tag{A.16}$$

And $\Gamma_{in} (i = 0,1,2,3)$ appearing in Eq. (39) are defined as

$$\begin{aligned}\Gamma_{0n} = \frac{\gamma_2(a)\xi_0 - \gamma_3(a)}{\gamma_1(a)} &\sqrt{\lambda_1} s_n \left[(c_{11} - \chi_1) \sqrt{\lambda_1} s_n I_0(s_n r_1) + (c_{12} - c_{11}) \frac{1}{r} I_1(s_n r_1) \right] \\ &- \xi_0 \sqrt{\lambda_2} s_n \left[(c_{11} - \chi_2) \sqrt{\lambda_2} s_n I_0(s_n r_2) + (c_{12} - c_{11}) \frac{1}{r} I_1(s_n r_2) \right] \\ &+ \sqrt{\lambda_3} s_n \left[(c_{11} - \chi_3) \sqrt{\lambda_3} s_n I_0(s_n r_3) + (c_{12} - c_{11}) \frac{1}{r} I_1(s_n r_3) \right]\end{aligned} \tag{A.17}$$

$$\begin{aligned}\Gamma_{in} = \frac{\gamma_2(a)\xi_i - \gamma_3(a)}{\gamma_1(a)} &\sqrt{\lambda_1} s_n \left[(c_{11} - \chi_1) \sqrt{\lambda_1} s_n I_0(s_n r_1) + (c_{12} - c_{11}) \frac{1}{r} I_1(s_n r_1) \right] \\ &- \xi_i \sqrt{\lambda_2} s_n \left[(c_{11} - \chi_2) \sqrt{\lambda_2} s_n I_0(s_n r_2)(c_{12} - c_{11}) \frac{1}{r} I_1(s_n r_2) \right] \\ &+ \sqrt{\lambda_i} s_n \left[(c_{11} + \chi_3) \sqrt{\lambda_i} s_n K_0(s_n r_i) - (c_{12} - c_{11}) \frac{1}{r} K_1(s_n r_i) \right] \quad (i = 1,2,3)\end{aligned} \tag{A.18}$$

References

Atsumi, A., Itou, S., 1974. Stresses in a transversely isotropic circular cylinder having a spherical cavity. Journal of Applied Mechanics, ASME 41 (2), 507–511.

Bland, D.R., 1961. Solutions of Laplace's Equation. Routledge and Kegan Paul Ltd., London.

Chau, K.T., Wei, X.X., 2000. Finite solid circular cylinders subjected to arbitrary surface load. Part I—Analytic solution. International Journal of Solids and Structures 37 (40), 5707–5732.

Ding, H.J., Chen, B., Liang, J., 1996. General solutions for coupled equations for piezoelectric media. International Journal of Solids and Structures 33 (16), 2283–2298.

Elliott, H.A., 1948. Three-dimensional stress distributions in hexagonal aeolotropic crystals. Proceeding of the Cambridge Philosophical Society 44, 522–533.

Hutchinson, J.R., 1972. Axisymmetric vibrations of a free finite-length rod. Journal of the Acoustical Society of America 51 (1), 233–240.

Hutchinson, J.R., 1980. Vibrations of solid cylinders. Journal of Applied Mechanics, ASME 47 (4), 901–907.

Kasano, H., Tsuchiya, H., Matsumoto, H., Nakahara, I., 1982. Stresses and deformations in a transversely isotropic hollow cylinder under a ring of radial load. Bulletin of the JSME 25 (200), 143–148.

Lekhnitskii, S.G., 1963. Theory of Elasticity of an Anisotropic Elastic Body English translation by P. Fern. Holden-Day Inc., San Francisco.

Levin, H.S., Klosner, J.M., 1967. Transversely isotropic cylinders under band loads. Journal of Engineering Mechanics, ASCE 93, 157–174.

Love, A.E.H., 1944. A Treatise on the Mathematical Theory of Elasticity. Dover, New York.

Matsuzaki, Y., 1997. Smart structures research in Japan (review article). Smart Materials and Structures 6, R1–R10.

Miklowitz, J., 1984. The Theory of Elastic Waves and Waveguides. North-Holland, Amsterdam.

Moghe, S.R., Neff, H.F., 1971. Elastic deformations of constrained cylinders. Journal of Applied Mechanics, ASME 38, 393–399.

Okumura, I.A., 1987. Generalization of Elliott's solution to transversely isotropic solids and its application. Structural Engineering/Earthquake Engineering 4 (2), 185–195.

Okumura, I.A., 1989. Stresses in a transversely isotropic, short hollow cylinder subjected to an outer band load. Archive of Applied Mechanics (Ingenieur Archiv) 59, 310–324.

Parton, V.Z., Kudryavtsev, B.A., 1988. Electromagnetoelasticity. Gordon and Breach, New York.

Paul, H.S., 1966. Vibrations of circular cylindrical shells of piezoelectric silver iodide crystals. Journal of the Acoustical Society of America 40 (5), 1077–1080.

Paul, H.S., Natarajan, K., 1994a. Axisymmetric free vibrations of piezoelectric finite hollow cylinder. in: Procedings of Third International Congress on Air- and Structure-borne Sound and Vibration, Montreal, Canada. pp. 1831–1838.

Paul, H.S., Natarajan, K., 1994b. Axisymmetric free vibrations of piezoelectric finite cylindrical bone. Journal of the Acoustical Society of America 96 (1), 213–220.

Pickett, G., 1944. Application of the Fourier method to the solution of certain boundary problems in the theory of elasticity. Journal of Applied Mechanics, ASME 11, A176–182.

Power, L.D., Childs, S.B., 1971. Axisymmetric stresses and displacements in a finite circular bar. International Journal of Engineering Science 9, 241–255.

Rajapakse, R.K.N.D., 1996. Electroelastic response of a composite cylinder with a piezoceramic core. In: Proceedings of SPIE Smart Materials and Structures Conference, vol. 2715. pp. 684–694.

Rajapakse, R.K.N.D., Zhou, Y., 1997. Stress analysis of piezoceramic cylinders. Smart Materials and Structures 6 (2), 169–177.

Vendhan, C.P., Archer, R.R., 1977. Axisymmetric stresses in transversely isotropic finite cylinders. International Journal of Solid and Structures 14, 305–318.

Wei, X.X., Chau, K.T., Wong, R.H.C., 1999. Analytic solution for axial point load strength test on solid circular cylinders. Journal of Engineering Mechanics, ASCE 125 (12), 1349–1357.

Wei, X.X., Chau, K.T., 2002. Analytic solution for finite transversely isotropic circular cylinders under the axial point load test. Journal of Engineering Mechanics, ASCE 128 (2), 209–219.